Appl Nanosci (2015) 5:297–303
DOI 10.1007/s13204-014-0317-2

ORIGINAL ARTICLE

Basella alba rubra spinach pigment-sensitized TiO_2 thin film-based solar cells

N. Gokilamani · N. Muthukumarasamy · M. Thambidurai · A. Ranjitha · Dhayalan Velauthapillai

Received: 6 January 2014 / Accepted: 5 May 2014 / Published online: 3 June 2014

Abstract Nanocrystalline TiO_2 thin films have been prepared by sol–gel dip coating method. The X-ray diffraction results showed that TiO_2 thin films annealed at 400, 450 and 500 °C are of anatase phase and the peak corresponding to the (101) plane is present in all the samples. The grain size of TiO_2 thin films was found to increase with increasing annealing temperature. The grain size is found to be 20, 25 and 33 nm for the films annealed at 400, 450 and 500 °C. The structure of the TiO_2 nanocrystalline thin films have been examined by high-resolution transmission electron microscope, Raman spectroscopy and FTIR spectroscopy. TiO_2 thin films were sensitized by natural dyes extracted from basella alba rubra spinach. It was found that the absorption peak of basella alba rubra extract is at about 665 nm. The dye-sensitized TiO_2-based solar cell sensitized using basella alba rubra exhibited a J_{sc} of 4.35 mA cm^{-2}, V_{oc} of 0.48 V, FF of 0.35 and efficiency of 0.70 %. Natural dyes as sensitizers for dye-sensitized solar cells are promising because of their environmental friendliness, low-cost production and fully biodegradable.

N. Gokilamani (✉) · N. Muthukumarasamy · A. Ranjitha
Department of Physics, Coimbatore Institute of Technology, Coimbatore, India
e-mail: gokilarajasekar@gmail.com

M. Thambidurai
Department of Electrical and Computer Engineering, Global Frontier Center for Multiscale Energy Systems, Seoul National University, Seoul 151-744, Republic of Korea

D. Velauthapillai
Department of Engineering, University College of Bergen, Bergen, Norway

Keywords Sol–gel · TiO_2 nanocrystalline thin film · Dye-sensitized solar cell

Introduction

Solar energy conversion based on dye sensitization of wide band gap nanocrystalline semiconductor films is an area of intense investigation (O'Regan and Gratzel 1991; Gratzel 2001; Hagfeldt et al. 1994). The most efficient dye-sensitized solar cells are based on ruthenium-centered polypyridyl metal organic complexes because of their strong absorption of visible light, favorable spatial separation of HOMO and LUMO states and because they can be repetitively oxidized and reduced without degradation (Nazeeruddin et al. 1993). Much of the research on natural sensitizers has focused on either chlorophyll or anthocyanin pigments. These have typically resulted in energy conversion efficiencies of <1 % (Cherepy et al. 1997; Dai and Rabani 2002; Kumara et al. 2006; Wongcharee et al. 2007; Polo and Murakami Iha 2006). The highest conversion efficiency for a dye-sensitized solar cell sensitized with a natural dye was 1.49 % obtained using chlorophyll-containing extracts from Rhoeo spathacea Stearn (Lai et al. 2008). Recently, 5.4 % conversion efficiency has been obtained by co-adsorption of two synthetic dyes obtained from chlorophyll precursors (Wang et al. 2010) which were extracted from plants. Another class of plant pigments with great potential for solar energy conversion is the betalains, consisting of the red betacyanins and yellow betaxanthins. Betalains are thought to serve the same functions in plants as anthocyanins, acting as "sunscreens" and antioxidants (Stintzing and Carle 2004; Heuer et al. 1994; Castellar et al. 2008). Recently, betacyanin class of plant pigments has been used in a dye-sensitized solar cell in which red

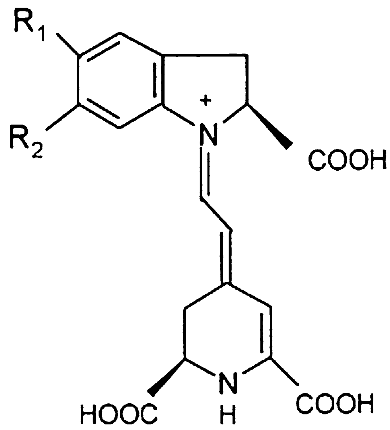

Fig. 1 The chemical structure of betacyanins molecules

beet root pigments were employed and energy conversion efficiency of 0.67 % has been reported (Zhang et al. 2008). The reddish-purple pigment betacyanin (Fig. 1) is commonly found in beets, bougainvillea flowers, prickly pear, etc., in most cases coexisting with another yellow or orange betaxanthin dye (Heuer et al. 1994; Castellar et al. 2008). Basella alba (family Basellaceae) known as Malabar spinach or cyclone spinach is a fast-growing vegetable, native of tropical Asia, probably originating from India or Indonesia. Basella alba rubra contains maximum betacyanin flavonoid. In this paper, betacyanin pigment extracted from basella alba rubra leaves are used to sensitize TiO_2 nanocrystalline thin films for dye-sensitized solar cells. A recent calculation shows that the visible transition of betacyanin is well-described as a HOMO → LUMO excitation which moves electron density from the aromatic ring to the dihydropyridyl moiety (Qin and Clark 2007).

Experimental

Fresh basella alba rubra spinach was cut into very small pieces and then soaked in 100 ml of ethanol at room temperature for 24 h and the solid residues were filtered out. The ethanol fraction was separated and few drops of concentrated HCl were added so that the solution became deep red in color (pH < 1). Then, the dye solution was stored at 4 °C before use. To prepare the photo-anode of dye-sensitized solar cells, the ITO conducting glass sheet (Asahi Glass; Indium-doped SnO_2, sheet resistance: 15 U/square) was first cleaned in a detergent solution using an ultrasonic bath for 15 min, rinsed with double-distilled water and then dried. The matrix sol was prepared by mixing 1.1 ml of titanium isopropoxide with 15 ml of isoproponal at room temperature and stirred for half an hour. Then 0.22 ml of glacial acetic acid is added drop wise and stirred vigorously for 2 h to obtain a homogeneous mixture of TiO_2 sol. The prepared sol was deposited on the ITO glass by sol–gel dip coating method. The film was dried at 80 °C for 30 min in air and then annealed at 400, 450 and 500 °C in a muffle furnace. The basella alba rubra spinach dye solution was used for sensitizing TiO_2 electrodes. The structural properties of the films have been studied using X-ray diffraction method (Rigaku Rint 2000 series). High-resolution transmission electron microscope (HRTEM) images of the prepared TiO_2 have been recorded using a JEOL JEM 2100 microscope. The absorption spectra of the films have been recorded using spectrophotometer (Jasco V-570). Lithium iodide, iodine and acetonitrile purchased from Sigma Aldrich have been used as received for the preparation of electrolyte. The redox electrolyte with $[I_3^-]/[I^-]$ 1:9 was prepared by dissolving 0.5 M LiI and 0.05 M I_2 in acetonitrile solvent. Since LiI is extremely hygroscopic, electrolytes were prepared in a dry room maintained at dew point of 60 °C. The counter electrode was prepared using platinum chloride as follows: the H_2PtCl_6 solution in isopropanol (2 mg ml^{-1}) was deposited onto the ITO glass by spin coating method. TiO_2 film annealed at 400, 450 and 500 °C has been used for the fabrication of solar cell. TiO_2 electrode was immersed in the extracted dye solution at room temperature for 24 h in the dark. The electrode was then rinsed with ethanol to remove the excess dye present in the electrode and then the electrode was dried. The counter electrode was placed on the top of the TiO_2 electrode, such that the conductive side of the counter electrode faces the TiO_2 film with a spacer separating the two electrodes. The two electrodes were clamped firmly together using a binder clip. Now, the prepared liquid electrolyte solution was injected into the space between the clamped electrodes. The electrolyte enters into the cell by capillary action. This resulted in the formation of sandwich-type cell. Natural dye-sensitized TiO_2-based solar cells have been fabricated with area of nearly 0.25 cm^2, and it was found that the cell efficiency was independent of cell area in this range as reported by Gokilamani et al. (2013). The J–V characteristic of the cell was recorded using a Keithley 4200-SCS meter. A xenon lamp source (Oriel, USA) with an irradiance of 100 mW cm^{-2} was used to illuminate the solar cell (equivalent to AM1.5 irradiation).

Results and discussion

TiO_2 nanocrystalline films have three well-known phases namely: anatase, rutile, and brookite. Rutile and anatase are tetragonal where as brookite is orthorhombic. Rutile is the only stable phase. Anatase and brookite are metastable at

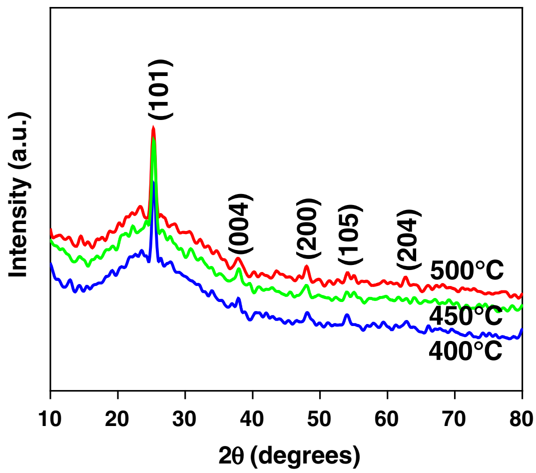

Fig. 2 X-ray diffraction pattern of TiO_2 thin films for different temperatures

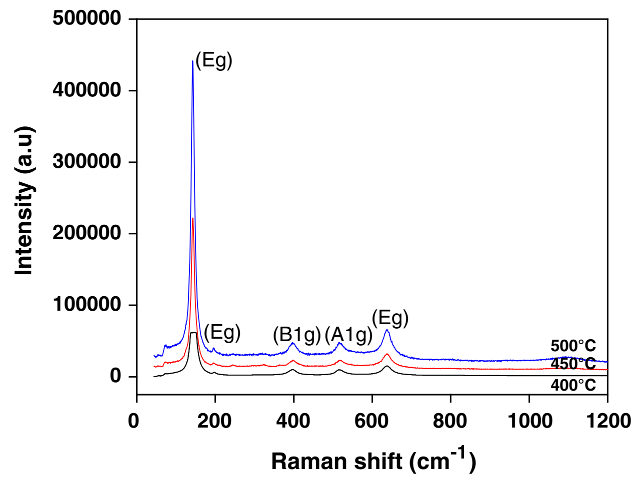

Fig. 3 The Raman spectra of TiO_2 thin film for different temperatures

all temperatures and can be converted to rutile after heat treatment at high temperatures (Lee et al. 2007). Figure 2 shows the diffraction pattern of the sol–gel prepared TiO_2 films, annealed at 400, 450 and 500 °C. A narrow peak at 25.35° corresponding to (101) reflection of the anatase phase of TiO_2 has been observed in the diffraction pattern (JCPDS No. 21-1272). The grain size has been calculated using Scherrer's formula (Culty 1978)

$$D = \frac{k\lambda}{\beta \cos \theta}$$

where D is the grain size, k is a constant taken to be 0.94, λ is the wavelength of the X-ray radiation, β is the full width at half maximum and θ is the angle of diffraction. The average grain size was found to be 20, 25 and 33 nm for the films annealed at 400, 450 and 500 °C, respectively. Grain size is found to increase with increase in annealing temperature. The annealing temperature facilitates the subsequent crystal growth process, accompanied by the diffusion of titania species forming big-sized anatase crystals and causing the merge of some adjacent mesopores. At the same time, the spatial confinement by mesopore arrays controls the formation and growth of anatase phase, leading to a more or less uniform distribution of titania nanocrystals (Que et al. 2006).

To discriminate the local order characteristics of the TiO_2 films, we carried out non-resonant Raman spectroscopy studies. The technique is non-destructive, capable to elucidate the titania structural complexity as peaks from each crystalline phase are clearly separated in frequency, and therefore the anatase and rutile phases are easily distinguishable. Figure 3 shows the Raman spectra of the nanocrystalline TiO_2 sample annealed at 400, 450 and 500 °C. Raman peaks originate from the vibration of molecular bonds, that is vibrational mode Eg and A1g peaks, which are related to different crystal planes. According to factor group analysis, anatase has six Raman active modes (A1g + 2B1g + 3Eg). Ohsaka (1980) have reported the Raman spectra of an anatase TiO_2 and have stated that six allowed modes appear at 144 cm^{-1} (Eg), 197 cm^{-1} (Eg), 399 cm^{-1} (B1g), 513 cm^{-1} (A1g), 519 cm^{-1} (B1g), and 639 cm^{-1} (Eg). The vibrational peaks of the nanocrystalline TiO_2 samples at 143 cm^{-1}, 197 cm^{-1}, 396 cm^{-1}, 519 cm^{-1}, 638 cm^{-1} and the absence of overlapped broad peaks show that the material is well crystallized, with low number of imperfect sites. These peaks are unambiguously attributed to the anatase modification. A special attention must be given to the Raman peaks observed at 143 cm^{-1}, 197 cm^{-1}, 396 cm^{-1}, 519 cm^{-1}, 638 cm^{-1} which are all slightly shifted, probably due to a smaller size of TiO_2 nanocrystalline particles (Arabatzis et al. 2002). There was no much shift in the peaks due to increase in temperature.

Fourier transform infrared (FTIR) spectroscopy is a promising method for observing molecular vibrations. Figure 4 shows the FTIR spectra of TiO_2 thin films annealed at 400, 450 and 500 °C. The thin films annealed at 400, 450 and 500 °C have peaks above 3,500 cm^{-1} which represents the O–H stretching of hydrogen bonds on the anatase TiO_2 surface. A reaction with a hydroxyl anion is thought of as the initial step of the photo oxidation of water. Since the TiO_2 sol layer has relatively small hardness and soft surface, it seems to be easy to dissociate the water or oxygen molecules from the sol surface. The hydrate water vibration peak at 1,550 cm^{-1} is still observed for all the three temperatures. This may be related to water bound to TiO_2 or may be due to the presence of reduced oxidant salt species or TiO_2 in a hydrate form (Xiaofeng et al. 2006). The films annealed at 400 °C exhibits a band at 3,718 cm^{-1} which is not observed for the films annealed at 450 and 500 °C, respectively, and this is

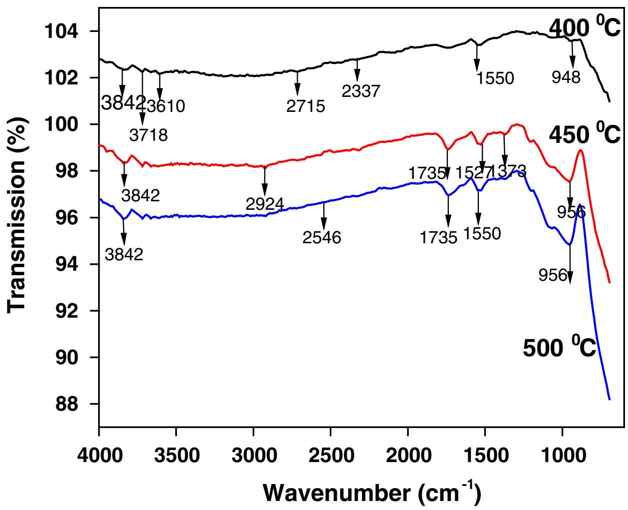

Fig. 4 The FTIR spectra of TiO_2 thin film for different temperatures

due to the removal of hydroxide group after annealing at higher temperatures. The intense band below 1,550 cm^{-1} is due to Ti–O–Ti vibrations. The slight shift of the band to the lower wave numbers and sharpening of the Ti–O–Ti band on annealing are may be due to the increase in size of the nanoparticles. In addition, the surface hydroxyl groups in TiO_2 increase with the increase of annealing temperature. Also, there are no additional bands present in the spectra corresponding to the alkoxy groups. This reveals that the addition of acetic acid has not introduced any residual impurities on the TiO_2 surface.

The atomic force microscope images of the prepared TiO_2 films annealed at 400, 450 and 500 °C are shown in Fig. 5a–c. The roughness of the TiO_2 film is found to be 18.8, 26.6 and 31.8 nm for the films annealed at 400, 450 and 500 °C, respectively. The mesoporous structure of TiO_2 film annealed at 500 °C was clearly observed from the AFM image. Figure 6a shows the closely packed agglomeration of the uniform nanoparticles in the mesoporous structure, which displays the even monodispersity of mesopores. This accumulation of nanoparticles creates narrow channels that may serve as electronic injection membranes (Cao et al. 2009). It can be seen from Fig. 6b that the size of the nanoparticles is extremely uniform. Figure 6c shows lattice fringes and the interplanar distance is measured to be 0.33 nm which corresponds to the (101) lattice plane of anatase phase of nanocrystalline TiO_2 thin films. Selective area electron diffraction pattern is used to learn about the crystal properties of a particular region. Figure 6d shows the selective area electron diffraction pattern of the nanocrystalline TiO_2 thin film and the presence of rings with discrete spots suggests that the TiO_2 nanocrystalline film is made of small particles of uniform size (Zheng et al. 2001).

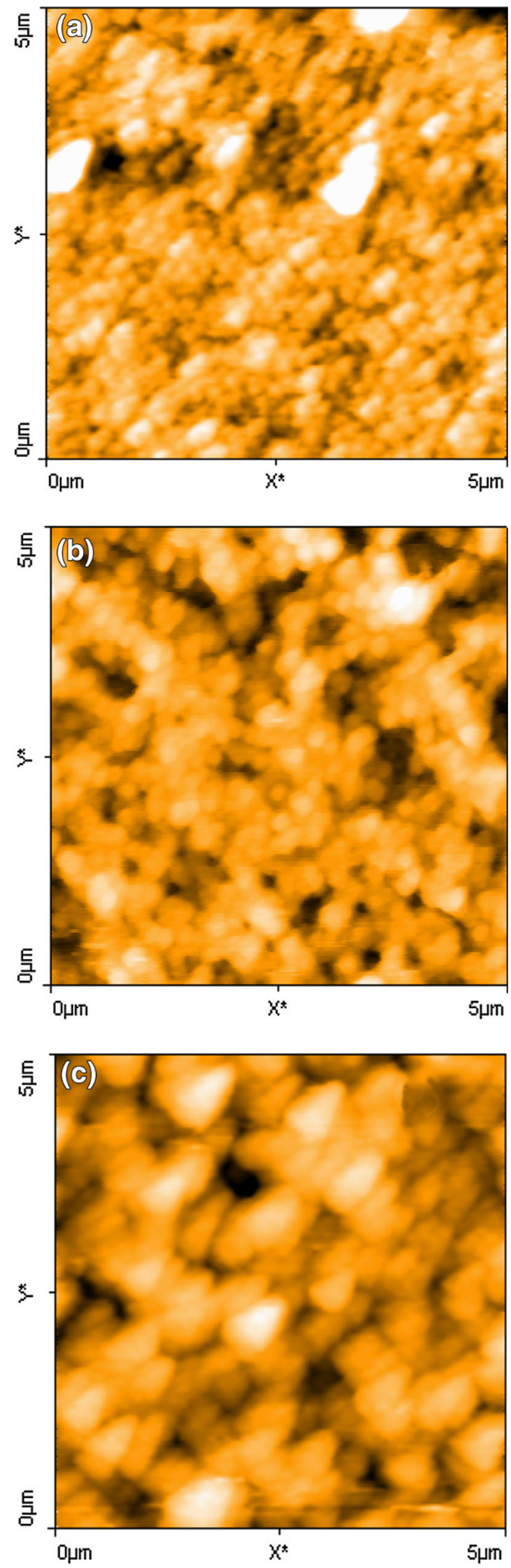

Fig. 5 AFM images of TiO_2 thin films annealed at **a** 400 °C, **b** 450 °C and **c** 500 °C

Fig. 6 HRTEM micrograph of TiO_2 nanocrystalline thin films annealed at 500 °C

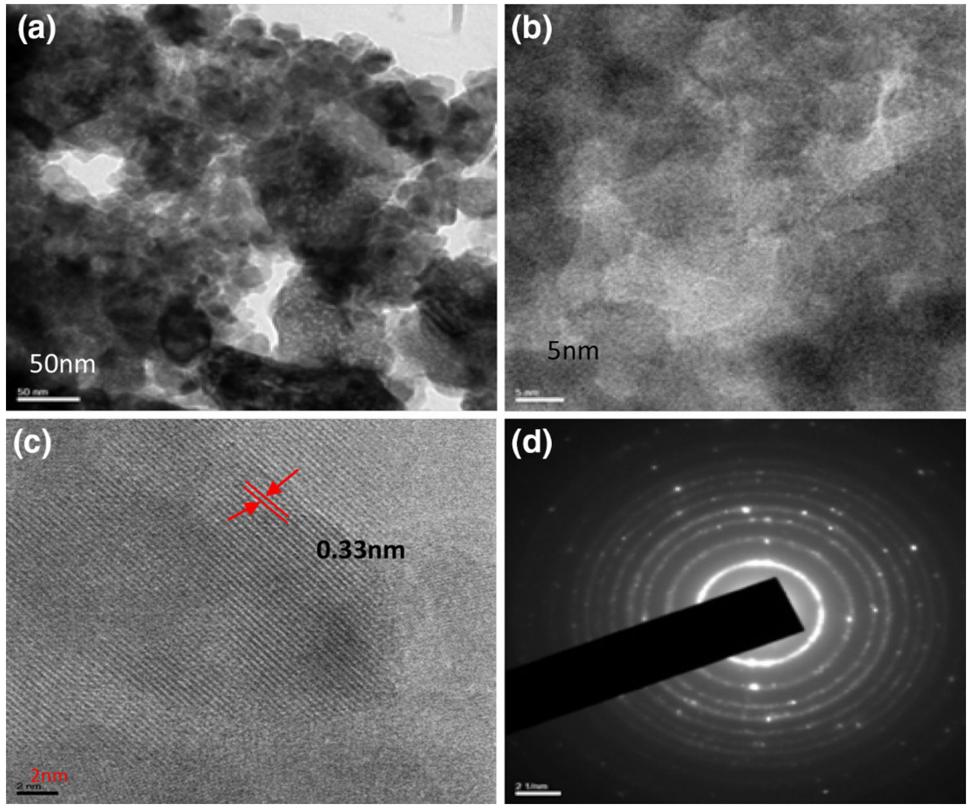

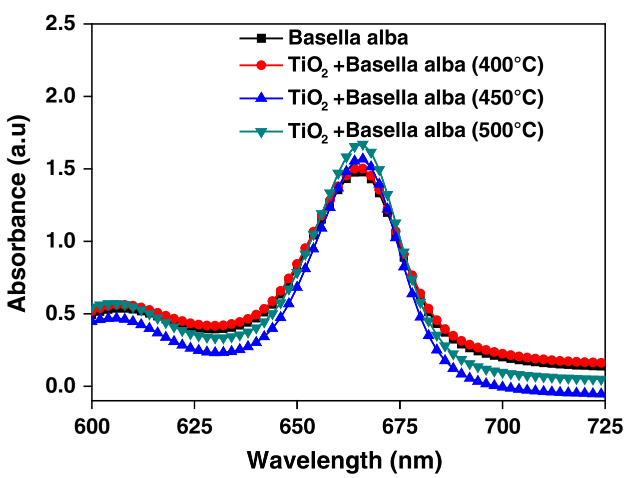

Fig. 7 Absorption spectra of basella alba rubra spinach-sensitized TiO_2 thin films for different temperatures

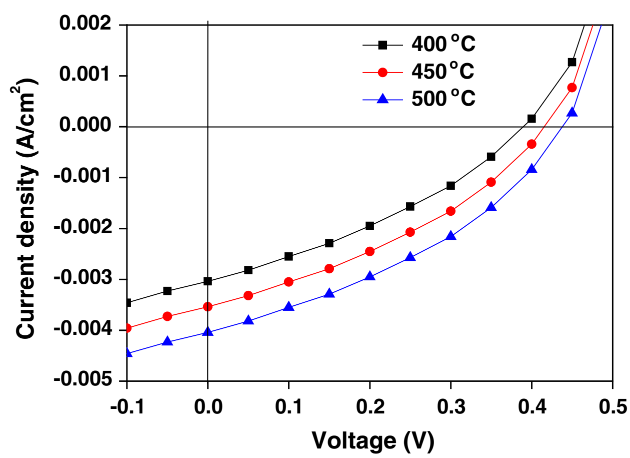

Fig. 8 J–V characteristics of dye-sensitized TiO_2-based solar cells for different temperatures

Optical absorption spectra of basella alba rubra and basella alba rubra-absorbed TiO_2 nanocrystalline thin films are shown in Fig. 7. It is seen that the absorption peak of basella alba rubra extract is maximum at 665 nm. The presence of the absorbance peak at 665 nm in basella alba rubra-sensitized TiO_2 nanocrystalline thin films confirms the incorporation of dye into the TiO_2 film. It is seen that absorption coefficients of basella alba rubra extract are about 19 times higher than that of the N-719 dye in high-efficiency dye-sensitized solar cells (Senthil et al. 2011). The intensity of light absorption has been enhanced due to the interfacial Ti–O coupling which exists between the C=O, C–H, $=CH_2$, O–H bonding of dye molecules and TiO_2 molecules.

The J–V characteristics of TiO_2 nanocrystalline thin films sensitized with natural dyes are shown in Fig. 8. The solar cell parameters, fill factor (FF) and efficiency (η), have been calculated using the following equations (Thambidurai et al. 2013, 2014, 2011)

$$\mathrm{FF} = J_{\mathrm{m}} \times V_{\mathrm{m}} / J_{\mathrm{sc}} \times V_{\mathrm{oc}}$$

$$\eta = (\mathrm{FF} \times J_{\mathrm{sc}} \times V_{\mathrm{oc}})$$

where J_{sc} is the short circuit photocurrent density (mA cm^{-2}), V_{oc} is the open circuit voltage (volts), P_{in} is the intensity of the incident light (100 W cm^{-2}) and J_{m} (mA cm^{-2}) and V_{m} (volts) are the maximum current density and voltage in the J–V curve, respectively, at point of maximum power output. The dye-sensitized solar cells with TiO_2 prepared at 400 °C show the power conversion efficiency (η) of 0.38 %, a short circuit current density (J_{sc}) = 3.06 mA cm^{-2}, open circuit voltage (V_{oc}) = 0.39 V and fill factor (FF) = 0.32. The dye-sensitized solar cell fabricated using TiO_2 prepared at 450 °C achieved a power conversion efficiency (η) of 0.50 % with a short circuit current density (J_{sc}) = 3.56 mA cm^{-2}, open circuit voltage (V_{oc}) = 0.41 V and fill factor (FF) = 0.34. The dye-sensitized solar cells with TiO_2 prepared at 500 °C exhibited a power conversion efficiency of 0.70 % with a short circuit current density (J_{sc}) of 4.35 mA cm^{-2}, open circuit voltage (V_{oc}) of 0.48 V and fill factor (FF) of 0.35. It was found that basella alba rubra extract possesses better photosensitization effect than betacyanin pigments from beets (Thambidurai et al. 2011).

Conclusion

TiO_2 nanocrystalline thin films have been prepared by a simple sol–gel method. X-ray diffraction analysis reveals that the TiO_2 nanocrystalline thin films exhibit anatase structure. The particle size seems to decrease with the increase of concentration of the precursor. The dyes extracted from basella alba rubra absorb visible light and have been found to be suitable for the use as sensitizer in solar cells. The efficiency of the fabricated dye-sensitized solar cell using basella alba rubra extract is 0.70 %.

References

Arabatzis IM, Antonaraki S, Stergiopoulos T, Hiskia A, Papaconstantinou E, Bernard MC, Falaras P (2002) Preparation, characterization and photocatalytic activity of nanocrystalline thin film TiO_2 catalysts towards 3,5-dichlorophenol degradation. J Photochem Photobiol A 149:237–245

Cao Y, Bai Y, Yu Q, Cheng Y, Liu S, Shi D, Gao F, Wang P (2009) Dye-sensitized solar cells with a high absorptivity ruthenium sensitizer featuring a 2-(hexylthio) thiophene conjugated bipyridine. J Phys Chem C 113:6290–6297

Castellar MR, Obon JM, Alacid M, Fernández-Lopez JA (2008) Fermentation of Opuntia stricta (Haw.) fruits for betalains concentration. J Agric Food Chem 56:4253–4257

Cherepy NJ, Smestad GP, Gratzel M, Zhang JZ (1997) Ultrafast electron injection: implications for a photoelectrochemical cell utilizing an anthocyanin dye-sensitized TiO_2 nanocrystalline electrode. J Phys Chem B 101:9342–9351

Culty BD (1978) Elements of X-ray diffraction. Addision-Wesley, New York

Dai Q, Rabani J (2002) Photosensitization of nanocrystalline TiO_2 films by anthocyanin dyes. J Photochem Photobiol A 26:421–429

Gokilamani N, Muthukumarasamy N, Thambidurai M, Ranjitha A, Velauthapillai D (2013) Utilization of natural anthocyanin pigments as photosensitizers for dye-sensitized solar cells. J Sol Gel Sci Technol 66:212–219

Gratzel Michael (2001) Photoelectrochemical cells. Nature 414(2001):338–344

Hagfeldt A, Didriksson B, Palmqvist T, Lindstrom H, Sodergren S, Rensmo H, Lindqist SE (1994) Verification of high efficiencies for the Gratzelcell, A 7 % efficient solar cell based on dye-sensitized colloidal TiO_2 films. Sol Energy Mater Sol Cells 31:481–488

Heuer S, Richter S, Metzger JW, Wray V, Nimtz M, Strack D (1994) Betacyanins from bracts of Bougainvillea glabra. Phytochemistry 37:761–767

Kumara GRA, Kaneko S, Okuya M, Onwana-Agyeman B, Konno A, Tennakone K (2006) Shiso leaf pigments for dye-sensitized solidstate solar cell. Sol Energy Mater Sol Cells 90:1220–1226

Lai WH, Su YH, Teoh LG, Hon MH (2008) Commercial and natural dyes as photosensitizers for a water-based dye-sensitized solar cell loaded with gold nanoparticles. J Photochem Photobiol A 195:307–313

Lee Kun-Mu, Suryanarayanan Vembu, Ho Kuo-Chuan (2007) A study on the electron transport properties of TiO_2 electrodes in dye-sensitized solar cells. Sol Energy Mater Sol Cells 91:1416–1420

Nazeeruddin MK, Kay A, Rodicio I, Humphry-Baker R, Muller E, Liska P, Vlachopoulos N, Gratzel M (1993) Conversion of light to electricity by cis-X2 bis(2,20-bipyridyl- 4, 40-dicarboxylate)ruthenium(II) charge-transfer sensitizers (X = Cl^{-}, Br^{-}, I^{-}, CN^{-}, and SCN^{-}) on nanocrystalline TiO_2 electrodes. J Am Chem Soc 115:6382–6390

O'Regan Brian, Gratzel Michael (1991) A low-cost, high-efficiency solar cell based on dye-sensitized colloidal TiO_2 films. Nature 353:737–740

Ohsaka Toshiaki (1980) Temperature dependence of the Raman Spectrum in Anatase TiO_2. J Phys Soc Jpn 48:1661

Polo AS, Murakami Iha NY (2006) Blue sensitizers for solar cells: natural dyes from Calafate and Jaboticaba. Sol Energy Mater Sol Cells 90:1936–1944

Qin C, Clark AE (2007) DFT characterization of the optical and redox properties of natural pigments relevant to dye-sensitized solar cells. Chem Phys Lett 438:26–30

Que W, Uddin A, Hu X (2006) Thin film TiO_2 electrodes derived by sol–gel process for photovoltaic applications. J power sources 159:353–356

Senthil TS, Muthukumarasamy N, Velauthapillai D, Agilan S, Thambidurai M, Balasundaraprabhu R (2011) Natural dye (cyanidin 3-O-glucoside) sensitized nanocrystalline TiO_2 solar cellfabricated using liquid electrolyte/quasi-solid-state polymer electrolyte. Renew Energy 36:2484–2488

Stintzing FC, Carle R (2004) Functional properties of anthocyanins and betalains in plants, food, and in human nutrition. Trends Food Sci Technol 15:19–38

Thambidurai M, Muthukumarasamy N, Velauthapillai D, Arul NS, Agilan S, Balasundaraprabhu R (2011) Dye-sensitized ZnO nanorod based photoelectrochemical solar cells with natural dyes extracted from Ixora coccinea, Mulberry and Beetroot. J Mater Sci Mater Electron 22:1662–1666

Thambidurai M, Muthukumarasamy N, Velauthapillai D, Lee C (2013) Synthesis and characterization of flower like ZnO nanorods for dye-sensitized solar cells. J Mater Sci Mater Electron 24:2367–2371

Thambidurai M, Muthukumarasamy N, Velauthapillai D, Lee C (2014) Rosa centifolia sensitized ZnO nanorods for photoelectrochemical solar cell applications. Sol Energy. doi:10.1016/j.solener.2014.01.045

Wang XF, Koyama Y, Kitao O, Wada Y, Sasaki S, Tamiake J, Zhou H (2010) Significant enhancement in the power-conversion efficiency of chlorophyll co-sensitized solar cells by mimicking the principles of natural photosynthetic light-harvesting complexes. Biosens Bioelectron 25:1970–1976

Wongcharee K, Meeyoo V, Chavadej S (2007) Dye-sensitized solar cell using natural dyes extracted from rosella and blue pea flowers. Sol Energy Mater Sol Cells 91:566–571

Xiaofeng Lu, Liu Xincai, Wang Lifeng, Zhang Wanjin, Wang Ce (2006) Fabrication of luminescent hybrid fibres based on the encapsulation of polyoxometalate into polymer matrices. Nanotechnology 17:3048–3053

Zhang D, Lanier SM, Downing JA, Avent JL, Lum J, McHale JL (2008) Betalain pigments for dye sensitized solar cells. J Photochem Photobiol A Chem 195:72–80

Zheng M-P, Gu M-Y, Jin Y-P, Wang H-H, Zu P-F, Tao P, He J-B (2001) Effects of PVP on structure of TiO_2 prepared by the sol–gel process. Mater Sci Eng B 87:197–201